Three-dimensional model study of the arctic ozone loss in 2002/2003 and comparison with 1999/2000 and 2003/2004

W. Feng, M. P. Chipperfield, S. Davies, B. Sen, G. Toon, J. F. Blavier, C. R. Webster, C. M. Volk, A. Ulanovsky, F. Ravegnani, et al.

Atmos. Chem. Phys. Discuss., 4, 5045–5074, 2004
www.atmos-chem-phys.org/acpd/4/5045/
SRef-ID: 1680-7375/acpd/2004-4-5045

Atmospheric Chemistry and Physics Discussions

Three-dimensional model study of the arctic ozone loss in 2002/2003 and comparison with 1999/2000 and 2003/2004

W. Feng[1], M. P. Chipperfield[1], S. Davies[1], B. Sen[2], G. Toon[2], J. F. Blavier[2], C. R. Webster[2], C. M. Volk[3], A. Ulanovsky[4], F. Ravegnani[5], P. von der Gathen[6], H. Jost[7], E. C. Richard[8], and H. Claude[9]

[1]Institute for Atmospheric Science, School of the Environment, University of Leeds, Leeds, UK
[2]NASA Jet Propulsion Laboratory, Pasadena, CA, USA
[3]J. W. Goethe University Frankfurt, Germany
[4]Central Aerological Observatory (CAO), Moscow, Russia
[5]Institute of Atmospheric Sciences and Climate (ISAC), Italian National Research Council, Bologna, Italy
[6]Alfred Wegener Institute, Potsdam, Germany
[7]NASA Ames, Moffett Field, CA, USA
[8]Aeronomy Laboratory, NOAA, Boulder, CO, USA
[9]Deutscher Wetterdienst, Germany

Received: 21 June 2004 – Accepted: 6 August 2004 – Published: 7 September 2004

Correspondence to: W. Feng (fengwh@env.leeds.ac.uk)

Abstract

We have used the SLIMCAT 3-D off-line chemical transport model (CTM) to quantify the Arctic chemical ozone loss in the year 2002/2003 and compare it with similar calculations for the winters 1999/2000 and 2003/2004. Recent changes to the CTM have improved the model's ability to reproduce polar chemical and dynamical processes. The updated CTM uses σ-θ as a vertical coordinate which allows it to extend down to the surface. The CTM has a detailed stratospheric chemistry scheme and now includes a simple NAT-based denitrification scheme in the stratosphere.

In the model runs presented here the model was forced by ECMWF ERA40 and operational analyses. The model used 24 levels extending from the surface to ~55 km and a horizontal resolution of either 7.5°×7.5° or 2.8°×2.8°. Two different radiation schemes, MIDRAD and the CCM scheme, were used to diagnose the vertical motion in the stratosphere. Based on tracer observations from balloons and aircraft, the more sophisticated CCM scheme gives a better representation of the vertical transport in this model which includes the troposphere. The higher resolution model generally produces larger chemical O_3 depletion, which agrees better with observations.

The CTM results show that very early chemical ozone loss occurred in December 2002 due to extremely low temperatures and early chlorine activation in the lower stratosphere. Thus, chemical loss in this winter started earlier than in the other two winters studied here. In 2002/2003 the local polar ozone loss in the lower stratosphere was ~40% before the stratospheric final warming. Larger ozone loss occurred in the cold year 1999/2000 which had a persistently cold and stable vortex during most of the winter. For this winter the current model, at a resolution of 2.8°×2.8°, can reproduce the observed loss of over 70% locally. In the warm and more disturbed winter 2003/2004 the chemical O_3 loss was generally much smaller, except above 620 K where large losses occurred due to a period of very low minimum temperatures at these altitudes.

ACPD

4, 5045–5074, 2004

1. Introduction

In recent years, three-dimensional (3-D) models have been widely used to study the behaviour of ozone and other constituents during winter in the Arctic and Antarctic (e.g. Brasseur et al., 1997). Many chemical transport models (CTMs), forced by meteorological analyses, can successfully reproduce the general features of the seasonal evolution of total column ozone. However, models still fail to reproduce many aspects of polar chemistry and transport. Moreover, given the large interannual variability in the Arctic it is important that any model is tested under different conditions.

Ozone loss in the Arctic stratosphere has received much attention over the past decade or so (e.g. see WMO, 2003). The significant year-to-year variability in Arctic meteorology leads to significant interannual variability in the polar ozone loss (Chipperfield and Jones, 1999). Thus, it is very difficult to determine the chemical ozone loss since it is masked by dynamic variability caused by reversible vertical and horizontal advection and by mixing of air masses (Grooß and Müller, 2003). In the past, many models have tended to underestimate the chemical O_3 loss during cold Arctic winters. Some of these also appear to overestimate the chemical loss during warm winters (e.g. Guirlet et al., 2000). Previous studies also indicate that current CTMs cannot give a satisfactory observed partial column ozone loss (e.g. Rex et al., 2004). All these conclusions are based on the fact that the CTMs cannot reproduce the observed ozone. In fact, successful quantitative simulation of ozone loss depends critically on the realistic combination of horizontal and vertical transport, chemistry, radiative transfer and other processes which must be correctly represented in the models.

In this paper we examine the performance of our recently updated SLIMCAT model in the Arctic stratosphere. We use it to investigate the Arctic chemical ozone loss in 2002/2003 and compared it with the winters 1999/2000 and 2003/2004. Section 2 describes the updated model and experiments performed. The different meteorological conditions related to the polar ozone loss for the three winters are presented in Sect. 3. Section 4 shows our model results including sensitivity studies to the different radiation

ACPD
4, 5045–5074, 2004

scheme and horizontal resolution. We also show how significant improvements were made in the new updated model when compared with observations especially for the cold Arctic winters 1999/2000 and 2002/2003. Section 5 summarises our conclusions.

2. Model and experiments

2.1. SLIMCAT 3-D CTM

SLIMCAT is an off-line 3-D CTM first described in Chipperfield et al. (1996). The original version of SLIMCAT used pure isentropic levels as a vertical coordinate and was thus limited to the domain above ~330 K (~9 km). The new version of SLIMCAT (Chipperfield, in preparation, 2004[1]) is now formulated using a hybrid σ-θ vertical coordinate, which means that it can extend down to the surface. Horizontal winds and temperatures are specified using meteorological analyses. Vertical advection is calculated from diabatic heating rates using a radiation scheme. The original SLIMCAT used the MIDRAD middle atmosphere radiation scheme (Shine, 1987) to determine the cross-isentropic flow since the lowest model vertical level was ~330 K. In this case the lower boundary to the radiation scheme was 700 hPa where climatological upwelling long-wave fluxes are specified in order to model reasonable heating rates above ~100 hPa. With the extension of the model to the surface the use of MIDRAD is likely no longer appropriate and we have added alternative radiation schemes including code based on the NCAR CCM (Briegleb, 1992). This scheme (hereafter called 'CCM') uses a δ-Eddington approximation (Joseph et al., 1976) and accurately computes absorbed solar radiation when compared to available reference calculations and observations (Briegleb, 1992). The downward and upward fluxes in the CCM radiation scheme can extend from 1000 hPa to the top of atmosphere.

[1]Chipperfield, M. P.: A new version of the TOMCAT/SLIMCAT off-line chemical transport model, Q. J. Roy. Met. Soc., in preparation, 2004.

Chemical tracers in SLIMCAT are advected using the scheme of Prather (1986) which conserves second-order moments. The model contains a detailed gas-phase stratospheric chemistry scheme (Chipperfield, 1999). The runs used here are based on photochemical data from JPL 2003 (Sander et al., 2003) with the exception of the absorption cross sections of Cl_2O_2 which were taken from Burkholder et al. (1990) extrapolated to 450 nm. The model also contains a treatment of heterogeneous reactions on liquid aerosols, nitric acid trihydrate (NAT) and ice (see Chipperfield, 1999). For the runs used here a simple NAT-based denitrification scheme was included in the model which assumes NAT forms in two modes. This is the same as the scheme described by Davies et al. (2002) and tested for the cold winter of 1999/2000.

2.2. Experiments

A series of full chemistry model runs were performed to investigate the performance of the updated SLIMCAT model (see Table 1). First, in runs A and B, SLIMCAT was initialised on 1 January 1989 and integrated at low horizontal resolution ($7.5^\circ \times 7.5^\circ$) for ~14 years using 6-hourly ECMWF analyses. These runs used ERA40 reanalyses from 1989 to 1999 and then operational analyses from 1 January 2000 onwards. The model used 24 levels from the surface to ~55 km with a resolution in the lower stratosphere of ~1.5–2 km. Run A used the MIDRAD radiation scheme while B used the CCM radiation scheme. The surface values of tropospheric source gases (CH_4, N_2O, halocarbons) were specified from WMO (2003) and an extra 100 pptv of chlorine was assumed to reach the stratosphere from short-lived Cl source gases (see WMO, 2003).

Output from these low resolution runs were taken and interpolated to a higher horizontal resolution ($2.8^\circ \times 2.8^\circ$) to initialise seasonal simulations for winters 1999/2000, 2002/2003 and 2003/2004. These seasonal runs were forced with ECMWF operational analyses throughout (runs C, D1, D2, E1 and E2, see Table 1). As well as providing the current best estimate of modelled polar O_3 depletion for these winters, these experiments investigate how the model radiation scheme and horizontal resolution affect

ACPD
4, 5045–5074, 2004

the calculation of chemistry and transport in the polar winter/spring.

3. Meteorology in the three arctic winters

The evolution of minimum temperatures is frequently used to provide an overview of the times favouring PSC formation (e.g. Manney et al., 1994; Feng et al., 2004). Figure 1 shows time series of minimum temperatures north of 50° N between 260–724 K (surface to ~28 km) from 1 December to late April in the years 1999/2000, 2002/2003 and 2003/2004. In the 1999/2000 winter, low temperatures ($T_{min} \leq 195$ K) occurred persistently above 450 K (~17 km) and descended with time reaching below 400 K (~14 km) in January. Minimum temperatures were below 185 K between 532–620 K (~22–26 km) during the period from late December to mid-January. The final stratospheric sudden warming occurred in late March. The year 2002/2003 can also be classed as a cold Arctic winter. Extremely low temperatures occurred from early December until mid-January and the coldest air around 6 December 2002 coincided with the area of an observed O_3 minihole around Scandinavia. Temperatures increased in late January then decreased again in early February. A stratospheric major sudden warming occurred in mid-February followed by a further cooling in late February and early March. The final warming began in late March. The 2003/2004 Arctic winter was warmer than these other years. Low temperatures ($T \leq 195$ K) occurred from 1 December to early January above 460 K (~18 km) and there was short cold period in late January. Another interesting point was the extremely cold period between mid February and mid March at higher altitudes above 620 K (~26 km). The analyses from United Kingdom Met Office (UKMO) (Swinbank and O'Neil, 1994) also captured the abnormal cold period for this winter (Y. Orsollini, personal communication, 2004).

Figure 1 (right) also shows the difference between minimum temperature and the equilibrium NAT formation temperature (T_{NAT}) in the polar region. Negative values of T-T_{NAT} show the possible PSC occurrence as a function of time and altitude. For these three winters, the altitude of possible PSCs gradually descended with time after

ACPD
4, 5045–5074, 2004

1 December. Clearly, PSCs occurred extensively during the 1999/2000 Arctic winter – a large reduction in PSCs occurred only after mid March 2000 due to the stratospheric warming. In 2002/2003 the main period of possible PSCs occurred from December 2002 until mid January 2003. Other occasional PSCs formation occurred around 8 February and 1 March 2003. However, much less PSC activity occurred in the winter 2003/2004.

Due to their long chemical lifetimes in the stratosphere nitrous oxide (N_2O) and methane (CH_4) can be used to study stratospheric dynamics. Their time evolution can provide information on the vertical and horizontal transport of air masses. Figure 2 shows the evolution of modelled N_2O and CH_4 (from the higher resolution seasonal simulations) at Ny-Ålesund station (79° N, 12° E) for the three winters 1999/2000, 2002/2003 and 2003/2004. Clearly, in 1999/2000 the vortex remained stable and located over Ny-Ålesund station for most of the winter. The disturbed vortex occurred only after 17 March 2000 due to the final stratospheric warming. In winter 2002/2003, the polar vortex was also stable before mid February but became more disturbed after that due to the major stratospheric sudden warming. The vortex returned over the station again from late February to mid March 2003 when the temperatures were again low. In contrast to the cold winters of 1999/2000 and 2002/2003, the polar vortex in 2003/2004 was much more disturbed for most of the time after January. Such a warm, disturbed polar vortex is not so conducive to large chemical ozone loss.

4. Results

4.1. Winter 1999/2000: comparison with ozone sondes

As a number of updates have been made to the SLIMCAT model we first compare it with O_3 sonde observations in 1999/2000. Previous studies with SLIMCAT have shown a good agreement between the model and the observed large depletion in the lower stratosphere in this cold winter (Sinnhuber et al., 2000). These older runs used

the purely θ-coordinate model and were forced by UKMO analyses. As discussed by Davies et al. (2002), although these simulations produce a realistic extent of chlorine activation (based on comparisons with in-situ aircraft data) this was partly due to denitrification caused by ice sedimentation which was facilitated by the erroneously cold UKMO temperatures for this winter. Similar simulations with ECMWF analyses for 1999/2000 did not give such large O_3 loss and the UKMO-forced model underestimated O_3 loss in previous cold winters (e.g. 1996/1997).

Figure 3 compares O_3 sonde observations at Ny-Ålesund with model runs for 1999/2000 (see Table 1). Clearly, the low resolution, multiannual run starting in 1989 using the MIDRAD radiation scheme (run A) underestimates the observed O_3 at the start of the winter (e.g. by ~0.5 ppmv at 460 K and 425 K in December). Run A gives a poor simulation for 1999/2000 Arctic winter. While the old (pure θ) version of SLIMCAT, with a lower boundary at 330 K was able to use MIDRAD successfully, the new model as used here extends down to the surface although MIDRAD was developed for use in the middle atmosphere only. MIDRAD cannot be expected to accurately calculate the upward radiative fluxes from the troposphere.

Figure 3 also shows results using the CCM radiation scheme. The O_3 simulation by the new version of SLIMCAT using the CCM radiation scheme (run B) clearly gives better results than run A. The calculated ozone in run B reproduces the observations in early December 1999 (after ten years of spin up) and successfully reproduces the large observed decrease in ozone at 425 K. However, this low resolution multiannual simulation overestimates the observed O_3 above 450 K after late February. The figure also shows the model passive ozone tracer. This is reset equal to the chemically integrated O_3 in early winter (1 January for run A and run B, see Table 1) and then advected passively without chemistry. At any point and time after that the difference between this passive O_3 and the model's chemically integrated O_3 tracer is the net chemical O_3 loss. Run A using MIDRAD calculates less polar ozone loss than run B using CCM radiation scheme.

A further significant improvement is made by the higher resolution (2.8°×2.8°) sea-

sonal simulation using the CCM radiation scheme (run C). The initialisation from run B is good and the higher resolution run captures the decrease up to day 70 better and also has lower O_3 when the vortex comes back over the station around day 90. Overall, run C, (forced by ECMWF analyses) successfully reproduces the observed ozone in the lower stratosphere for the cold Arctic winter 1999/2000. The effect of the model radiation scheme and resolution is discussed in more detail in Sects. 4.2 and 4.4.

4.2. High latitude descent: Comparison with balloon and aircraft data for 2002/2003

The differences in the model results for runs A and B, which differ only in the scheme used to diagnose vertical transport, clearly indicate the need to test these runs against tracer observations. Some balloon and aircraft observations are available for the winter 2002/2003 and many more are available for winter 1999/2000.

Figure 4 shows profiles observed by the MkIV balloon instrument (Toon, 1991) on 16 December 2002 along with SLIMCAT output from the higher resolution simulations for 2002/2003 winter (run D1 and run D2). The profiles of long-lived species N_2O and CH_4 can be used to verify the modelled tracer transport. Downward transport is strongly underestimated by the SLIMCAT run using MIDRAD (run D2). The model run using the CCM radiation scheme (run D1) gives more descent than run D2. Simulations using the more realistic CCM radiation scheme for diagnosing diabatic descent (run D1) more accurately reproduces the observed ozone profile from the MkIV balloon than the MIDRAD scheme (run D2).

Comparisons with in-situ aircraft observations during 2002/2003 also show similar results. Figure 5 shows an example of one M55 Geophysica flight for 26 January 2003. The Geophysica aircraft flew at between ~18 km and ~20 km, corresponding to ~450 K and ~500 K. The aircraft dived to ~14 km when it reached northward of 75° N. The operational ECMWF temperatures used in the model compare well with observations. The transport, in particular the descent of air masses, is well reproduce by the model using CCM radiation scheme (run D1) when compared with the observed N_2O measured on board the M55 by the HAGAR instrument (Volk et al., 2000; Riediger

ACPD
4, 5045–5074, 2004

et al., 2000). The similar results from other flights comparisons (not shown here) also indicate that the model run using MIDRAD radiation scheme (run D2) underestimates the descent of air masses. Reasonable diabatic descent also gives a better simulation of ozone. Figure 5 also shows that ~0.5–0.7 ppmv ozone loss occurred at 18 km and ~0.6 ppmv loss at 20 km from run D1. Less ozone loss is diagnosed from run D2. Therefore, different vertical descent of air masses in the polar vortex can significant affect vertical transport of ozone.

Figure 6 compares the higher resolution model with the CCM radiation scheme with tracer data from winter 1999/2000. The data comes from the ER-2 flight of 11 March 2000 where the aircraft flew inside the polar vortex near the start and at the end of the flight (Konopka et al., 2004). The model reproduces the magnitude of observed N_2O and CH_4 inside the vortex, as well as the gradient at the vortex edge. This supports the conclusion that this model setup gives a realistic representation of transport in the lower stratosphere.

4.3. Arctic O_3 loss in 2002/2003 and 2003/2004: comparison with sondes

Figure 7 shows a comparison of the $2.8^\circ \times 2.8^\circ$ resolution SLIMCAT simulations with O_3 sondes at Ny-Ålesund for Arctic winter 2002/2003. The results from the low resolution simulations (run A and B) are not shown here as the results are similar to Fig. 3. For this year there is only a small difference (<0.1 ppmv) in the early December ozone value between runs D1 and D2 (initialised from runs A and B, respectively). after 13 years run. However, the winter/spring evolution of ozone using different radiation schemes is again very different.

The run using the CCM radiation scheme (run D1) is in good agreement with ozone observations for winter 2002/2003. The observed sudden change in ozone around mid February and mid March in the lower stratosphere is due to the stratospheric sudden warming and more disturbed polar vortex (see Figs. 1 and 2). The large observed decrease in ozone around mid February below 460 K (~18 km) is due to the vortex moving away from Ny-Ålesund and is characteristic of mid-latitude air.

ACPD
4, 5045–5074, 2004

The higher resolution run D1 still shows large loss (~1.1 ppmv) in the lower stratosphere in the winter 2002/2003. Interestingly, earlier ozone loss in December 2002 also can be seen here if compared with 1999/2000 Arctic winter. Figure 4 shows that the Mk IV balloon instrument detected evidence for Cl activation on the flight of 16 December 2002 around 23 km. This supports the model results of activation and O_3 loss, although in the model the HCl removal extends over a deeper region.

Figure 8 shows the equivalent comparison of ozone in the 2003/2004 Arctic winter. The observed O_3 levels in 2003/2004 are larger than the other colder winters discussed here (i.e. 1999/2000 and 2002/2003 in Figs. 3 and 7). Overall, the higher resolution SLIMCAT simulation reproduces the observed O_3 levels in the lower stratosphere well for the warm and disturbed winter 2003/2004, but there is noticeable discrepancy around the period when the vortex becomes more weak and disturbed (days 55 and 70). Model results show about 0.6 ppmv ozone loss at 460 K between 1 December and the end of March.

4.4. Chlorine activation: Effect of meteorology and model resolution

Figure 9 (left) shows the modelled ClO_x (=ClO+2Cl_2O_2) at Ny-Ålesund as a function of time and θ for three years. Here the results are from the 2.8°×2.8° resolution model using the CCM radiation scheme. For the three winters, chlorine activation occurred from early December and activation gradually descended consistent with the corresponding low temperatures and likely PSC extent (Fig. 1). In the year 2002/2003, much more chlorine activation occurred in early December and even extended down to 400 K around 6 December. A more rapid deactivation followed the major warming after mid February (not shown). Then reactivation occurred during the period from late February to mid March 2003 due to the cooling of polar air masses and potential PSCs occurrence. The chlorine activation on PSCs lasted longer in the year 1999/2000 due to the persisting stable polar vortex and lower temperatures. In contrast, in 2003/2004 the activation occurred over a much shorter period and at higher levels from early December until late January.

ACPD
4, 5045–5074, 2004

The right panels in Fig. 9 show the equivalent plots from the low resolution multi-annual run B. The features are generally similar to the higher resolution runs. The differences in ClO_x in December 1999 near 600 K are due to the different analyses used in the two experiments during this month: run B used ERA40 analyses until 1 January 2000 while run C used the operational analyses. Late on in this winter (i.e. early March) the ClO_x values in the higher resolution run persist with higher values. Figure 10 shows that the higher concentrations of ClO_x are partly due to higher Cl_y concentrations, caused by stronger descent and less mixing, and partly due to the stronger denitrification found in the higher resolution run.

The different chlorine activation determines the different ozone loss. Figure 11 shows the local % ozone loss at Ny-Ålesund station for the three modelled winters. Obviously, larger ozone depletion occurred in the year of 1999/2000, due to more denitrification which reduced chlorine deactivation to $ClONO_2$. Ozone loss in the warm 2003/2004 winter is generally much smaller, but abnormally large above 620 K due to the period of very low minimum temperatures above this altitude. In 2002/2003 the local maximum ozone loss at Ny-Ålesund was about 40% of the initial 1 December value before the final warming. Figure 11 also shows that early local ozone loss occurred in December due to more activation on PSCs and extremely low temperatures.

Figure 12 shows time series of averaged chemical ozone loss at 465 K and partial column ozone loss (~10–26 Km) between equivalent latitudes 65°–90° N. The averaged polar O_3 loss is less than the local ozone loss at Ny-Ålesund shown above. At 456 K there is an average ~25% chemical O_3 loss by the end of March for 2002/2003 and about 10% ozone loss for 2003/2004, with no further ozone loss after mid February 2003. The maximum polar ozone loss in the year 1999/2000 reached about 40% at 456 K. The figure again shows the early chemical loss in December 2002 due to the low temperature and early chlorine activation. The partial column (~10 to 26 km) ozone chemical loss reached 15 DU by the end of December and about 65 DU by the end of March in the winter 2002/2003. In the year 1999/2000, larger chemical ozone loss occurred and reached about 100 DU by the end of March. While less chemical ozone

ACPD
4, 5045–5074, 2004

loss occurred in the warm and more disturbed winter 2003/2004, the partial column ozone loss between 345 K–670 K is about 40 DU by the end of March 2004.

4.5. Comparison with midlatitude O_3 sonde data

For the 3 winter studies we show a brief comparison with ozone observations at mid-latitudes. Figure 13 shows comparison of O_3 between sonde observations and high-resolution simulations at Hohenpeißenberg (48° N, 11° E) for the three winters (see Table 1). The observed O_3 at middle latitudes is clearly larger in 2003/2004 than for the other two years. A significant changes in ozone were observed at Hohenpeißenberg in the three years at 460 K. However, the model shows that these are dynamical effects – the difference between the model O_3 and the passive O_3 (not shown) is still very small in this period.

5. Conclusions

We have used the recently updated SLIMCAT 3-D off-line CTM to study Arctic ozone loss in winter 2002/2003 and compare it with the very cold winter of 1999/2000 and the warm, disturbed winter 2003/2004. The different radiation schemes and horizontal resolution used in the model results in different tracer transport and polar ozone loss. For the new version of SLIMCAT used here, which extends down to the surface, the more detailed CCM radiation scheme produces more accurate tracer transport in the cold winters 1999/2000 and 2002/2003 and produces a better simulation in mid-latitude region. The higher resolution model gives more reasonable transport and mixing than the lower resolution.

The CTM results show that very early chemical ozone loss occurred in December 2002 due to extremely low temperatures and early chlorine activation in the lower stratosphere. Thus, chemical loss in this winter started earlier than in the other two winters studied here. In 2002/2003 the local polar ozone loss in the lower stratosphere

ACPD
4, 5045–5074, 2004

was ∼40% before the stratospheric final warming. Larger ozone loss occurred in the cold year 1999/2000 which had a persistently cold and stable vortex during most of the winter. For this winter the current model, at a resolution of 2.8°×2.8°, can reproduce the observed loss of over 70% locally. In the warm and more disturbed winter 2003/2004 the chemical O_3 loss was generally much smaller, except above 620 K where large losses occurred due to the period of very low minimum temperatures at these altitudes.

Overall, the best version of the updated model presented here gives a realistic representation of O_3 and inferred O_3 loss for a selection of winters. This is an advance over earlier versions of our model and other published studies, and shows that our ability to reproduce polar ozone loss is becoming more quantitative.

Acknowledgements. We are grateful for use of the VINTERSOL campaign data. This work was supported by the UK Natural Environment Research Council and by the EU TOPOZ III and QUILT projects. The ECMWF analyses were obtained via the British Atmospheric Data Centre. We thank M. Evans for useful discussions.

References

Brasseur, G. P., Tie, X., and Rasch, P. J.: A three-dimensional simulation of the Antarctic ozone hole: Impact of anthropogenic chlorine on the lower stratosphere and upper troposphere, J. Geophys. Res., 102, 8909–8930, 1997.

Briegleb, B. P.: Delta-Eddington Approximation for Solar Radiation in the NCAR Community Climate Model, J. Geophys. Res., 97, 7603–7612, 1992.

Burkholder J. B., Orlando, J. J., and Howard, C. J.: Ultraviolet-absorption cross-sections of Cl_2O_2 between 210 and 410 nm, J. Phys. Chem., 94, 687–695, 1990.

Chipperfield, M. P.: Multiannual simulations with a three-dimensional chemical transport model, J. Geophys. Res., 104, 1781–1805, 1999.

Chipperfield, M. P.: A three-dimensional model study of long-term mid-high latitude lower stratosphere ozone changes, Atmos. Chem. Phys., 3, 1–13, 2003.

Chipperfield, M. P. and Jones, R. L.: Relative influences of atmospheric chemistry and transport on Arctic O_3 trends, Nature, 400, 551–554, 1999.

Chipperfield, M. P., Santee, M. L., Froidevaux, L., Manney, G. L., Read, W. G., Waters, J. W., Roche, A. E., and Russell, J. M.: Analysis of UARS data in the southern polar vortex in September 1992 using a chemical transport model, J. Geophys. Res., 101, 18 861–18 881, 1996.

Davies, S., Chipperfield, M. P., Carslaw, K. S., Sinnhuber, B. M., Anderson, J. G., Stimpfle, R. M., Wilmouth, D. M., Fahey, D. W., Popp, P. J., Richard, E. C., von der Gathen, P., Jost, H., and Webster, C. R.: Modeling the effect of denitrification on Arctic ozone depletion during winter 1999/2000, J. Geophys. Res., doi:10.1029/2001JD000445, 2002.

Feng, W., Chipperfield, M. P., Roscoe, H. K., Remedios, J. J., Waterfall, A. M., Stiller, G. P., Glatthor, N., Hopfner, M., and Wang, D.-Y.: Three-Dimensional Model Study of the Antarctic Ozone Hole in 2002 and Comparison with 2000, J. Atmos. Sci., in press, 2004.

Grooß, J.-U. and Müller, R.: The impact of mid-latitude intrusions into the polar vortex on ozone loss estimates, Atmos. Chem. Phys., 3, 395–402, 2003.

Guirlet, M., Chipperfield, M. P., Pyle, J. A., Goutail, F., Pommereau, J. P., and Kyro, E.: Modeled Arctic ozone depletion in winter 1997/1998 and comparison with previous winters, J. Geophys. Res., 105, 22 185–22 200, 2000.

Hanson, D. and Mauersberger, K.: Laboratory studies of the nitric acid trihydrate: Implications for the south polar stratosphere, Geophys. Res. Lett., 15, 855–858, 1988.

Joseph, J. H., Wiscombe, W. J., and Weinman, J. A.: The Delta-Eddington approximation for radiative flux transfer, J. Atmos. Sci., 33, 2452–2459, 1976.

Konopka, P., Steinhorst, H.-M., Grooß, J.-U., Günther, G., Müller, R., Elkins, J., Jost, H.-J., Richard, E., Schmidt, U., Toon, G., and McKenna, D. S.: Mixing and ozone loss in the 1999–2000 Arctic vortex: Simulations with the three-dimensional Chemical Lagrangian Model of the Stratosphere (CLaMS) J. Geophys. Res., 109, doi:10.1029/2003JD003792, 2004.

Manney, G. L., Froidevaux, L., Waters, J. W., et al.: Chemical depletion of ozone in the Arctic lower stratosphere during winter 1992–93, Nature, 370, 429–434, 1994.

Prather, M. J.: Numerical advection by conservation of second-order moments, J. Geophys. Res., 91, 6671–6681, 1986.

Rex, M., Salawitch, R. J., von der Gathen, P., Harris, N. R. P., Chipperfield, M. P., and Naujokat, B.: Arctic ozone loss and climate change, Geophys. Res. Lett., 31, L04116, doi:10.1029/2003GL018844, 2004.

Riediger, O., Volk, C. M., Strunk, M., and Schmidt, U.: HAGAR – a new in situ tracer instrument for stratospheric balloons and high altitude aircraft, Eur. Comm. Air Pollut. Res. Report, 73,

727–730, 2000.
Sander, S. P., Ravishankara, A. R., Friedl, R. R., et al.: Chemical kinetics and photochemical data for use in stratospheric modeling, Update to Evaluation no. 12, JPL Publ., 00-3, 2003.
Shine, K. P.: The middle atmosphere in the absence of dynamical heat fluxes, Q. J. R. Meteorol. Soc., 113, 603–633, 1987.
Sinnhuber, B. M., Chipperfield, M. P., Davies, S., Burrows, J. P., Eichmann, K. U., Weber, M., von der Gathen, P., Guirlet, M., Cahill, G. A., Lee, A. M., and Pyle, J. A.: Large loss of total ozone during the Arctic winter of 1999/2000 Geophys. Res. Lett., 27, 3473–3476, 2000.
Swinbank, R. and O'Neill, A.: A stratosphere-troposphere data assimilation system, Mon. Weather Rev., 122, 686–702, 1994.
Toon, G.: The JPL MKIV interferometer, Opt. Photonics News, 2, 19–21, 1991.
Volk, C. M., Riediger, O., Strunk, M., Schmidt, U., Ravegnani, F., Ulanovsky, A., and Rudakov, V.: In situ tracer measurements in the tropocal tropopause region during APE-THESEO, Eur. Comm. Air Pollut. Res. Report, 73, 661–664, 2000.
World Meteorological Organization (WMO): Scientific assessment of ozone depletion: 2002, Global Ozone Res. Monit. Proj. Rep., 45, UNEP/WMO, Geneva, Switzerland, 2003.

Table 1. SLIMCAT model experiments.

Run	Resolution	Radiation Scheme	Dates	Initialisation	Passive ozone reset
A	7.5°×7.5°	MIDRAD	01/01/1989–28/04/2004		1 January
B	7.5°×7.5°	CCM	01/01/1989–04/04/2004		1 January
C	2.8°×2.8°	CCM	01/12/1999–19/04/2000	B	1 December
D1	2.8°×2.8°	CCM	01/12/2002–20/04/2003	B	1 December
D2	2.8°×2.8°	MIDRAD	01/12/2002–19/04/2003	A	1 December
E1	2.8°×2.8°	CCM	01/12/2003–19/04/2004	B	1 December
E2	2.8°×2.8°	MIDRAD	01/12/2003–05/04/2004	A	1 December

ACPD
4, 5045–5074, 2004

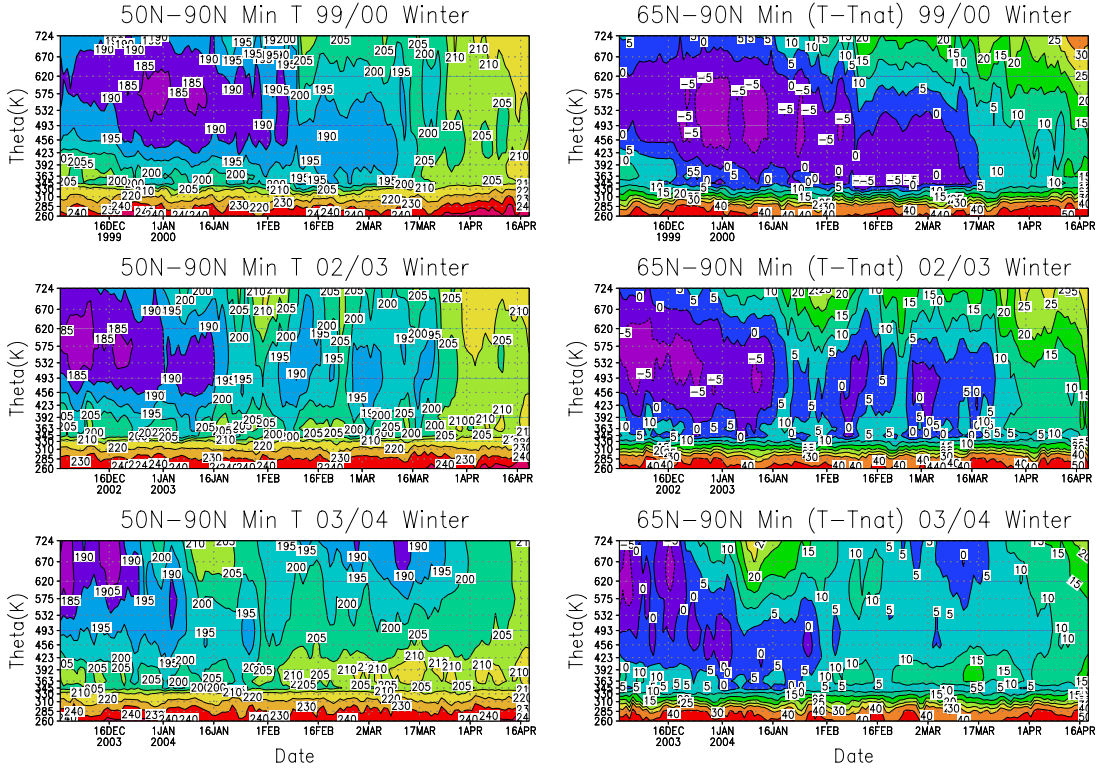

Fig. 1. The evolution of minimum temperature (K) northward of 50° N (left) and minimum difference between temperature and the equilibrium NAT formation temperature (T-T_{NAT}, K) northward of 65° N (right) as a function of time and θ in Arctic winters 1999/2000, 2002/2003, and 2003/2004. T_{NAT} was calculated based on model H_2O and HNO_3 using the expression of Hanson and Mauersberger (1988).

ACPD
4, 5045–5074, 2004

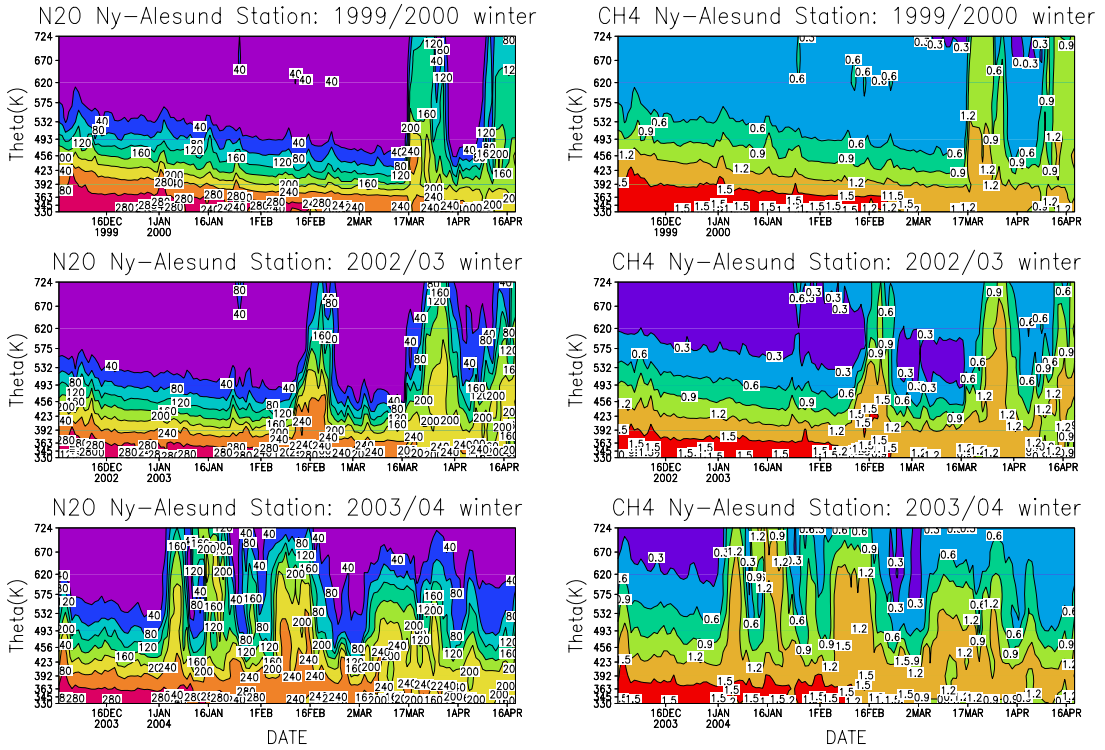

Fig. 2. Model N_2O (ppbv) and CH_4 (ppmv) at Ny-Ålesund station (79° N, 12° E) from SLIMCAT runs C, D1, and E1 as a function of time and θ for the three Arctic winters (top: 1999/2000, middle: 2002/2003, bottom: 2003/2004).

ACPD
4, 5045–5074, 2004

Arctic ozone loss in SLIMCAT 3-D CTM

W. Feng et al.

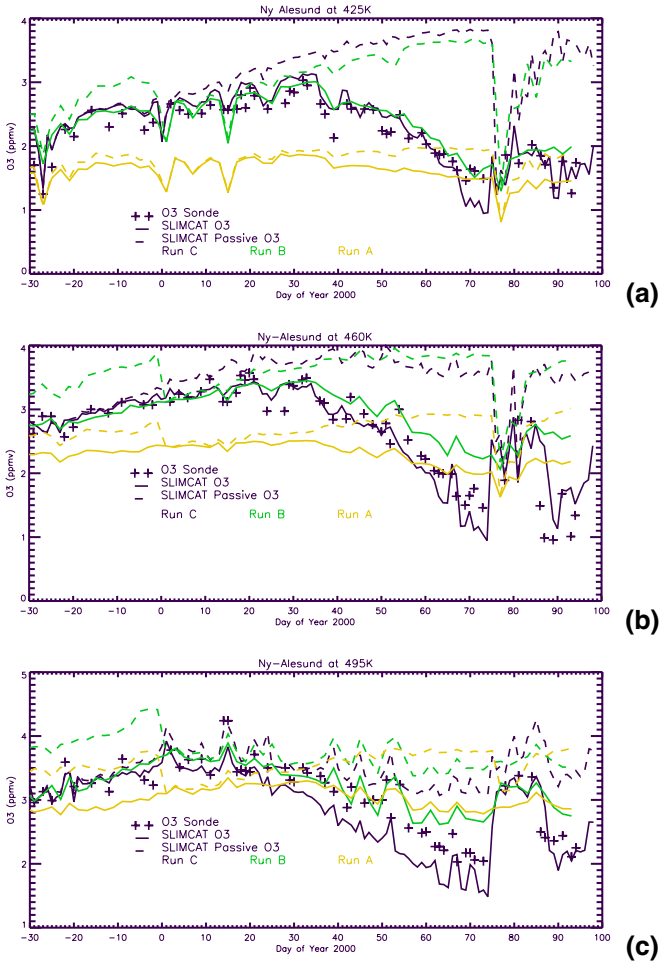

Fig. 3. Comparison of O_3 sonde observations (+ marks) at Ny-Ålesund for 1999/2000 with results for SLIMCAT runs A (yellow), B (green) and C (blue) for θ levels **(a)** 425 K, (**b)** 460 K and **(c)** 495 K. The dashed lines indicate the passive model O_3 tracer.

ACPD
4, 5045–5074, 2004

Arctic ozone loss in SLIMCAT 3-D CTM

W. Feng et al.

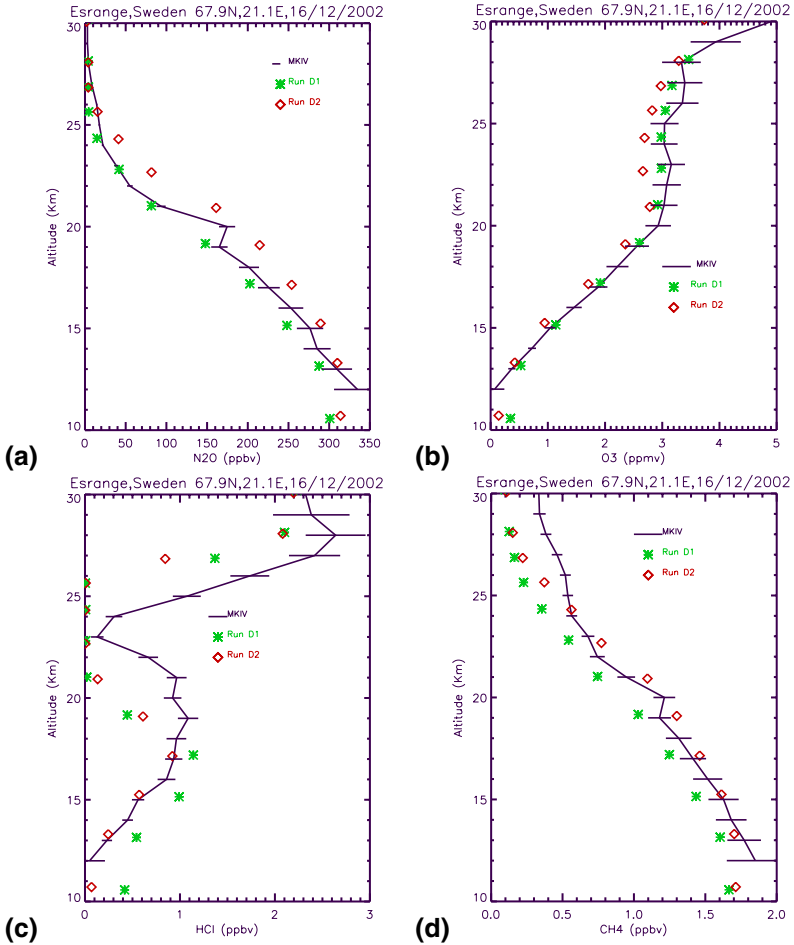

Fig. 4. MkIV balloon observations of **(a)** N_2O (ppbv), **(b)** O_3 (ppmv), **(c)** HCl (ppbv) and **(d)** CH_4 (ppmv) at Esrange (68° N, 21° E) on 16 December 2002 along with results from SLIMCAT model runs D1 (green) and D2 (red).

ACPD
4, 5045–5074, 2004

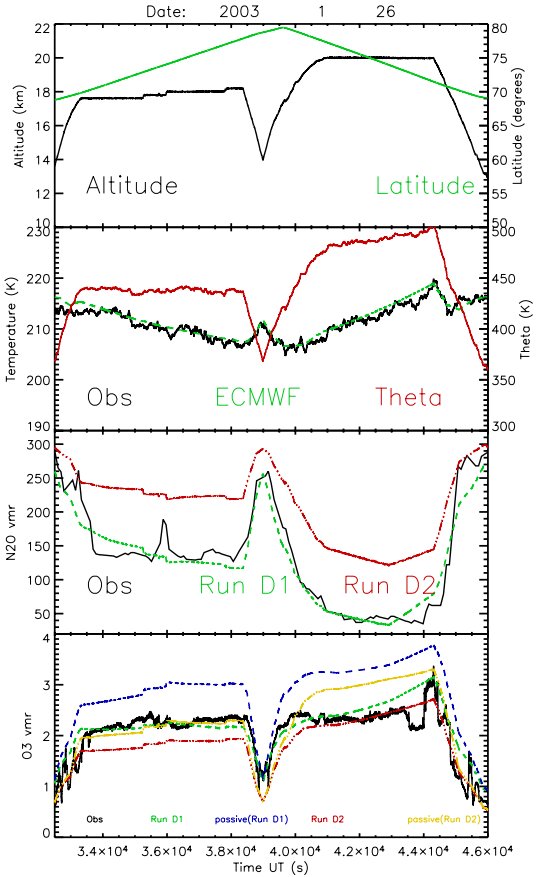

Fig. 5. Observations from the M55 Geophysica flight of 26 January 2003 compared with SLIMCAT model runs. **(a)** Latitude and altitude of flight track. **(b)** Observed and model (ECMWF) temperature and calculated θ. **(c)** Observed HAGAR N_2O (solid black line) and model results from runs D1 (CCM) and D2 (MIDRAD). **(d)** Observed FOZAN O_3 (solid black line) and model O_3 and passive O_3 from runs D1 (CCM) and D2 (MIDRAD).

ACPD
4, 5045–5074, 2004

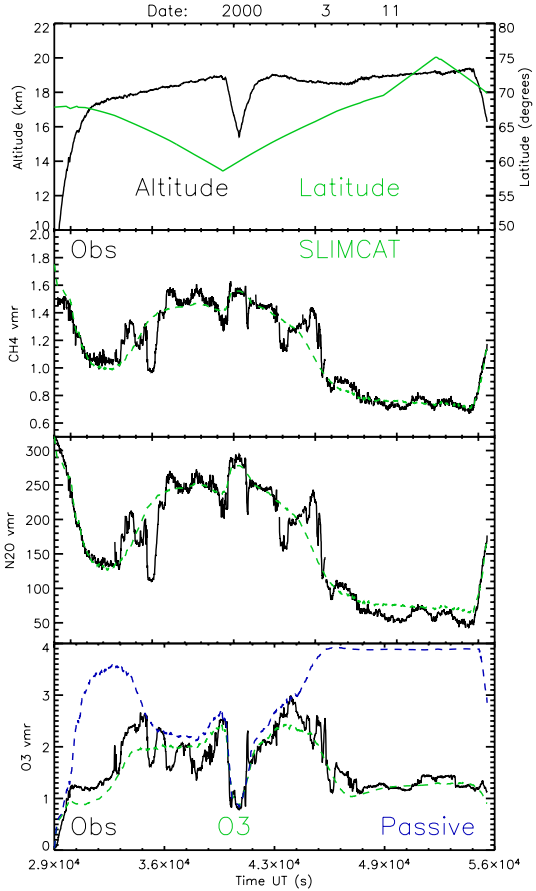

Fig. 6. Observations from the ER-2 flight of 11 March 2000 compared with SLIMCAT model run C. **(a)** Latitude and altitude of flight track. **(b)** Observed and modelled CH_4. **(c)** Observed and modelled N_2O. **(d)** Observed and model O_3 along with passive O_3 (blue).

ACPD
4, 5045–5074, 2004

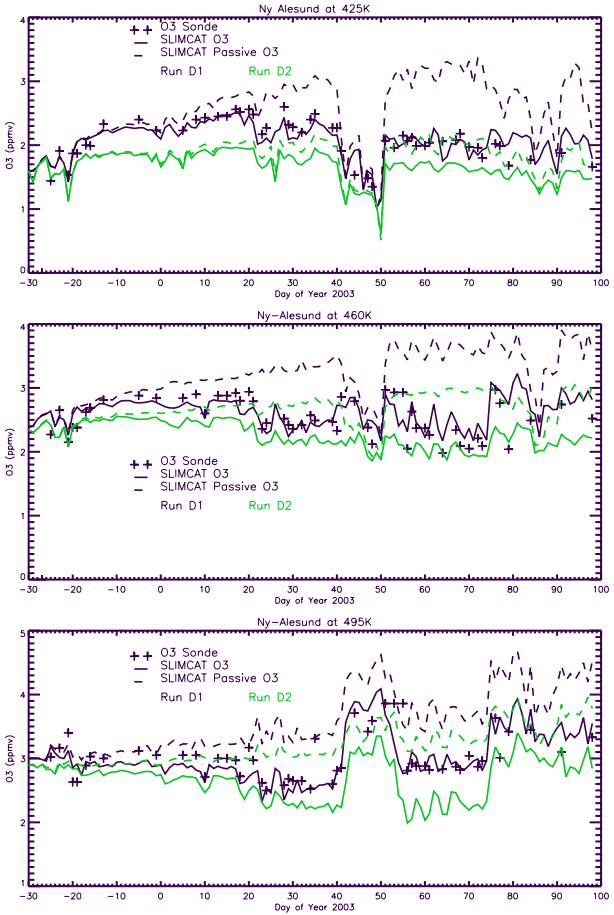

Fig. 7. Comparison between O_3 sonde observations (+) at Ny-Ålesund and results from the 2.8°×2.8° resolution SLIMCAT runs D1 (black) and D2 (green) for winter 2002/2003 (top: 425 K, middle: 460 K, bottom: 495 K).

ACPD
4, 5045–5074, 2004

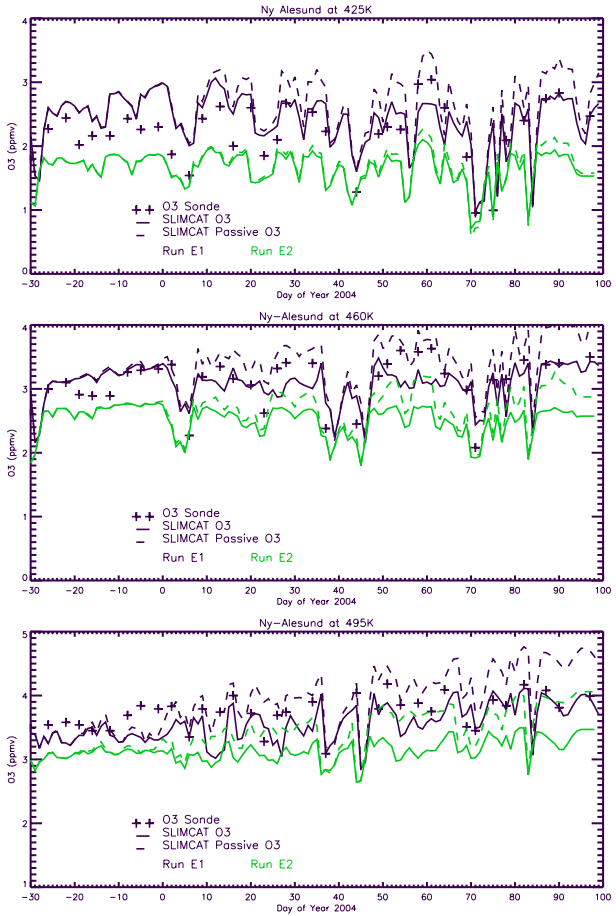

Fig. 8. Same as Fig. 7 but for Arctic winter 2003/2004.

ACPD
4, 5045–5074, 2004

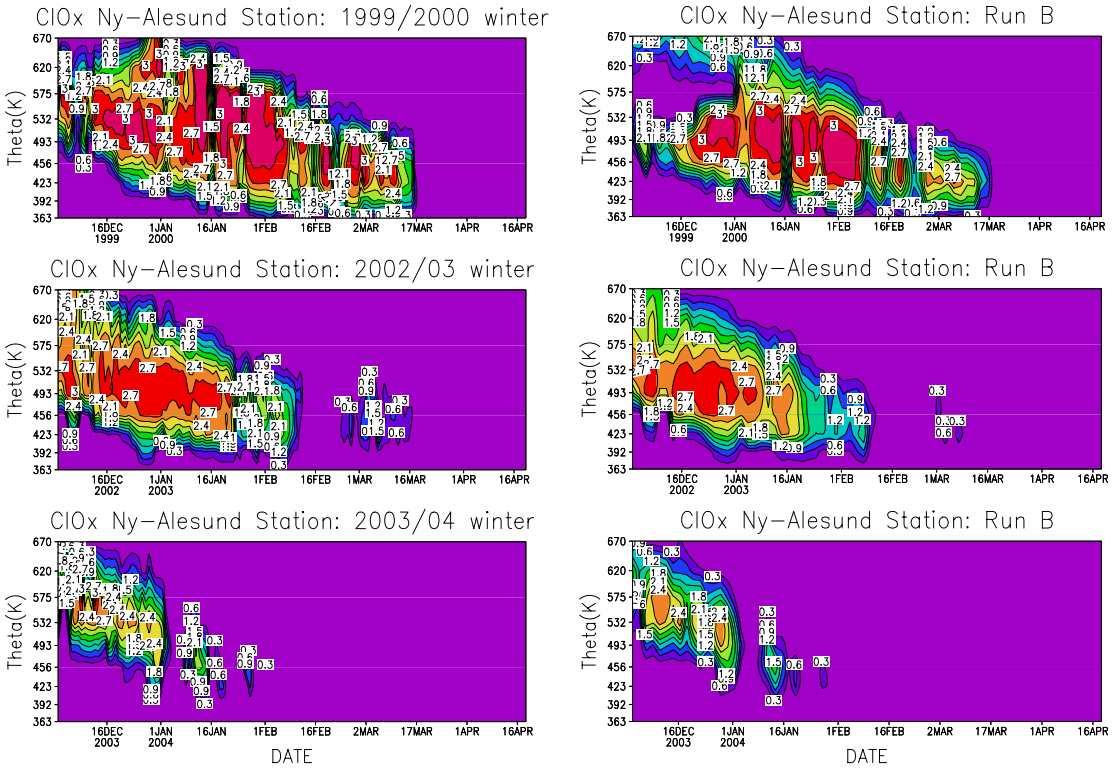

Fig. 9. Modelled ClO_x (=ClO+2Cl_2O_2) (ppbv) at Ny-Ålesund (79° N, 12° E) for the Arctic winters 1999/2000 (top), 2002/2003 (middle) and 2003/2004 (bottom). The left panels show results from the higher resolution runs (top run C, middle run D1 and bottom run E1) and the right panels show results from the low resolution multiannual run B.

ACPD
4, 5045–5074, 2004

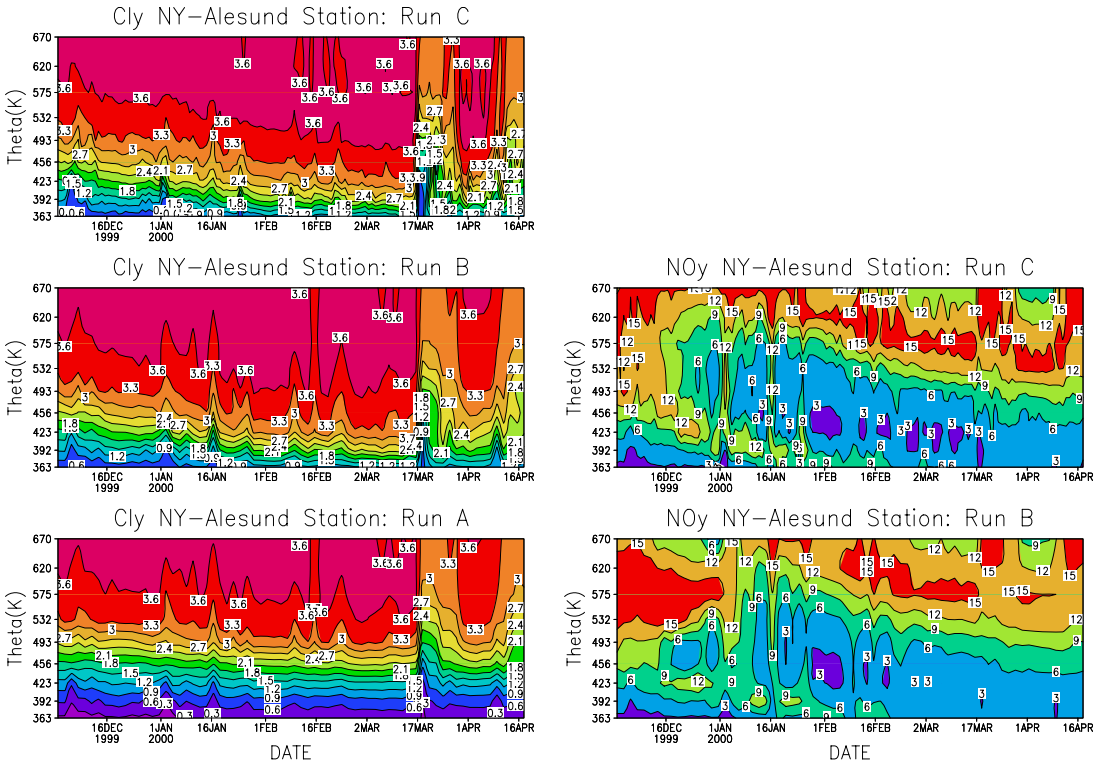

Fig. 10. Modelled Cl_y (ppbv, left) and NO_y (ppbv, right) at Ny-Ålesund (79° N, 12° E) for the Arctic winters 1999/2000 for run C (top), run B (middle) and run A (lower – Cl_y only).

ACPD
4, 5045–5074, 2004

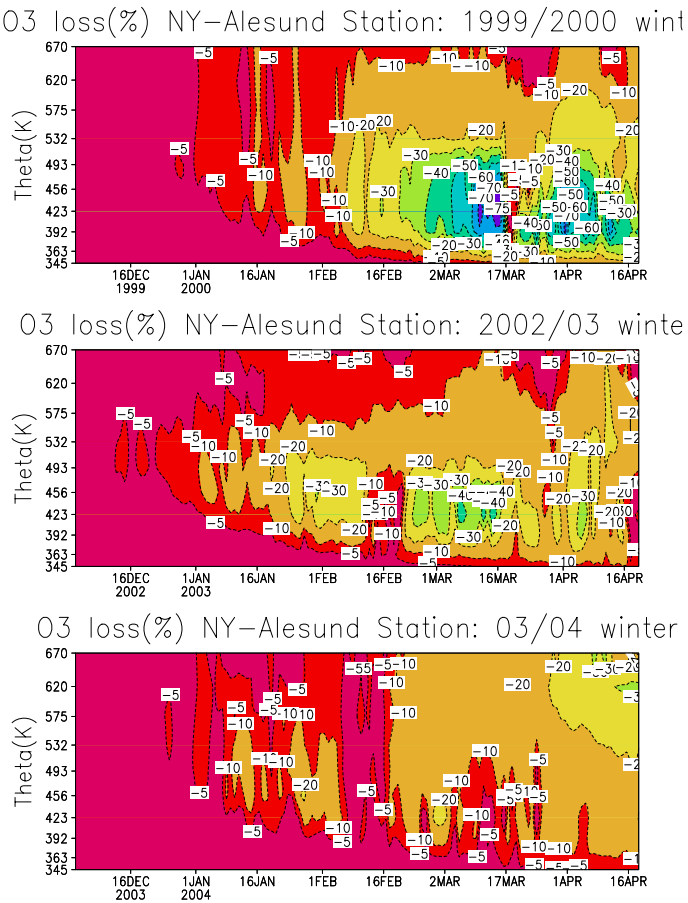

Fig. 11. As Fig. 9 (left), but for % local ozone loss.

ACPD
4, 5045–5074, 2004

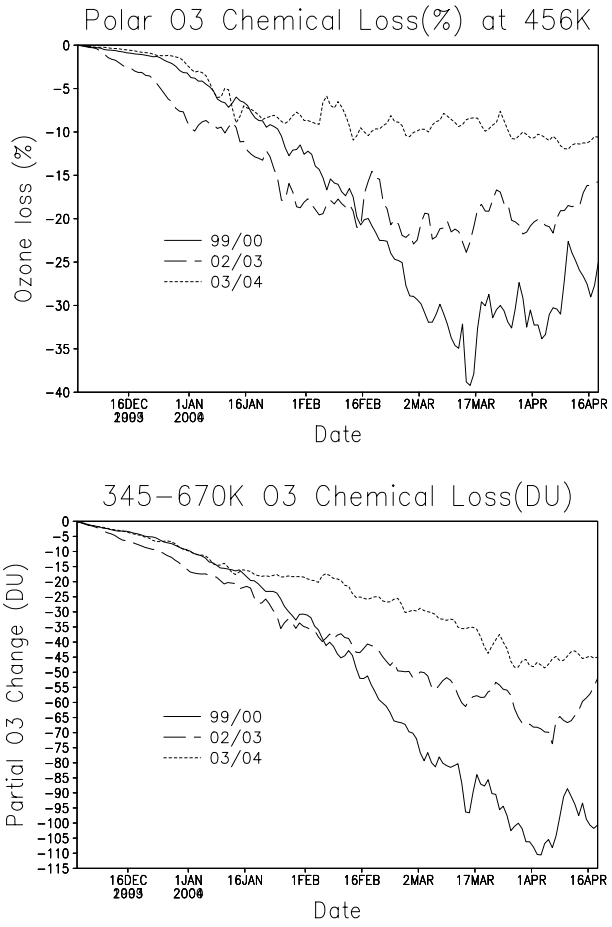

Fig. 12. Time series of averaged chemical ozone loss for **(a)** 465 K (%) and **(b)** 10 to 26 km partial column (DU) between equivalent latitudes 65°–90° N.

ACPD
4, 5045–5074, 2004

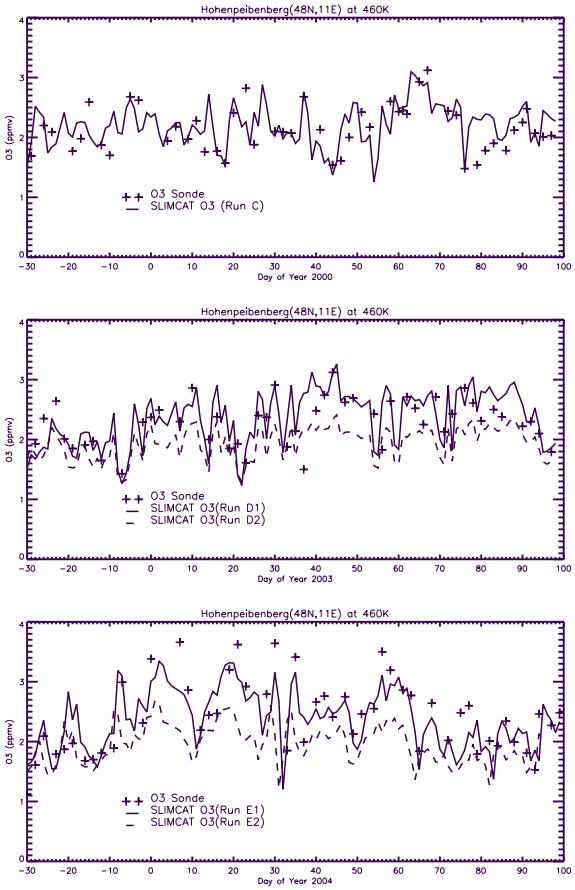

Fig. 13. Comparison of ozone sonde observations (+) at 460 K at Hohenpeißenberg (48° N, 11° E) with SLIMCAT 2.8°×2.8° resolution simulations for three Arctic winters (top: 1999/2000, middle: 2002/2003, bottom: 2003/2004). The solid lines use the CCM radiation scheme and the dashed lines use the MIDRAD radiation scheme.

ACPD
4, 5045–5074, 2004